



Verification of the ΔK_{eff} hypothesis along the fatigue crack path in thin and thick Al specimens

Julián Andrés Ortiz González, Jaime Tupiassú Pinho de Castro, Giancarlo Luis Gomez Gonzáles, Marco Antonio Meggiolaro, José Luiz de França Freire

Pontifical Catholic University of Rio de Janeiro, PUC-Rio, R. Marquês de São Vicente 225, Rio de Janeiro, 22451-900, Brazil
 julian@aluno.puc-rio.br, jtcastro@puc-rio.br, gonzalessglg@aaa.puc-rio.br, meggi@puc-rio.br, jlfreire@puc-rio.br

ABSTRACT. Elber assumed that the actual driving force for fatigue crack growth (FCG) is the effective stress intensity factor ΔK_{eff} . His hypothesis is verified here by means of easily reproducible tests. To do so, both DC(T) and C(T) specimens are cut from a 6351-T6 Al alloy 76mm diameter circular bar with two different thicknesses, 2 and 30mm, tested under fixed ΔK and K_{max} to simulated plane stress and plane strain FCG conditions. A strain-gage bonded on the back face of the specimens is used to measure the crack length and a custom-made Labview program is used to control the applied load, maintaining ΔK and K_{max} constant along the crack path. Moreover, the crack opening load is redundantly measured during the FCG tests, using far field strains from the back face gage and near field strains from a series of gages bonded along the crack path, as well as an independent digital image correlation system to measure displacement/strain fields on the face of the specimens. These tests show that the Al specimens reproduce the behavior previously observed in similar tests in 1020 steel: a significant decrease of the opening load as the cracks grow along the specimens, while maintaining a FCG rate essentially constant under the fixed $\{\Delta K, K_{\text{max}}\}$ loading, a behavior that cannot be explained by the ΔK_{eff} hypothesis.

KEYWORDS. Fatigue crack growth driving forces, crack opening force measurements, ΔK_{eff} limitations.



Citation: González J.A.O., Castro J.T.P., Gonzáles G.L.G., Meggiolaro M.A., Freire J.L.F., Verification of the ΔK_{eff} hypothesis along the fatigue crack path in thin and thick Al specimens, *Frattura ed Integrità Strutturale*, xx (2018) ww-zz.

Received: xx.yy.zzzz

Accepted: xx.yy.zzzz

Published: xx.yy.zzzz

Copyright: © 2019 This is an open access article under the terms of the CC-BY 4.0, which permits unrestricted use, distribution, and reproduction in any medium, provided the original author and source are credited.

INTRODUCTION

Monitoring the stiffness curve of a fatigue cracked plate during its loading cycle, Elber identified in the early 70's that "as a consequence of the permanent tensile plastic deformation left in the wake of a fatigue crack, one should expect partial crack closure after unloading the specimen" [1], as illustrated in Fig. 1. Having clearly identified experimentally that fatigue cracks can remain partially closed even under tensile loads ("the crack will not be totally opened until reaching the



magnitude of the opening load (P_{op})), the so-called plasticity-induced crack closure (PICC) behavior, he then assumed that “the crack cannot propagate while it is closed at its tip” [2]. Therefore, based on this hypothesis, Elber suggested that the effective stress intensity factor (SIF) range ΔK_{eff} should be the actual fatigue crack growth (FCG) driving force, instead of, for instance, $\{\Delta K, K_{max}\}$ or the equivalent $\{\Delta K, R\}$ combinations. By definition, $\Delta K_{eff} = K_{max} - K_{op}$ if $K_{op} > K_{min}$, or else $\Delta K_{eff} = \Delta K$ if $K_{op} < K_{min}$, where K_{max} and K_{min} are the maximum and the minimum values of the applied SIF, K_{op} is the SIF that completely opens the fatigue crack, and $R = K_{min}/K_{max}$.

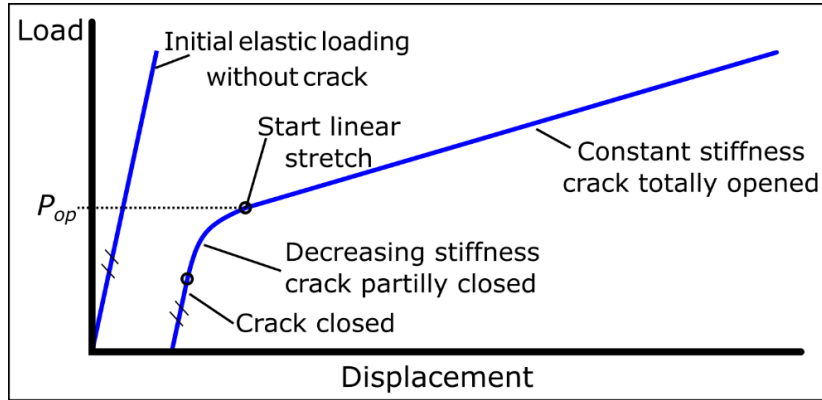


Figure 1: Load vs. displacement stiffness curve, used to determine the crack opening load P_{op} .

In other words, Elber assumed that FCG rates da/dN should be a function of ΔK_{eff} , $da/dN = f(\Delta K_{eff})$, because cracks could not grow before completely opening their tips, supposing that only under $K > K_{op}$ they would be further exposed to the loads. This hypothesis certainly is reasonable. In fact, PICC can justify many load sequence effects in FCG, such as delays or arrests after overloads (OL), attenuation of OL-induced delay effects after subsequent underloads, and FCG threshold sensitivity to R , which can much affect fatigue life estimates under variable amplitude loads (VAL). Hence, it is not surprising that FCG models based on ΔK_{eff} concepts still are very much used in practical applications [3-4].

However, although many experiments (including the data presented here) support the existence of PICC, see e.g. [5-7], its actual role in FCG is still controversial, to say the least. Indeed, albeit successful in explaining many FCG peculiarities, Elber’s hypothesis that ΔK_{eff} is the FCG driving force cannot explain many other equally important FCG characteristics, such as:

- (i) delays or arrests after OLs under high- R base loads (when fatigue cracks remain always open, since for such loads $K_{min} > K_{op}$) [8].
- (ii) constant FCG rates induced by constant $\{\Delta K, R\}$ but highly variable ΔK_{eff} loadings, observed in the data presented here for an Al alloy and in previous works for a low-C steel [9-10].
- (iii) cracks arrested at $R = 0.3$ that restart to grow at $R = 0$ under the same ΔK_{eff} [11]; or else.
- (iv) FCG threshold insensitivity to R in inert environments [12].

For further details in those and other ΔK_{eff} limitations, see for instance [3-4, 8, 13]. Notice that such limitations are supported by plenty of experimental data, so they are not based only on heuristic or philosophical arguments. It is not the aim of this work to explore the many FCG idiosyncrasies that cannot be properly explained by the ΔK_{eff} hypothesis, but it is not possible to ignore they exist. In fact, it is a truism to say that as dogmas have no place in science, all scientific hypotheses need proper experimental support, and ΔK_{eff} is no exception to this rule. Thus, it is not realistic to assume that PICC is the single or even the dominant mechanism in all FCG problems. Prudent structural designers should be aware that ΔK_{eff} -based FCG life predictions can be questioned based on such issues.

Anyway, for this work purposes, it suffices to say that ΔK_{eff} limitations can be very important for practical FCG life estimates. Indeed, if the effective SIF is not the actual FCG driving force, predictions based on it might be highly unreliable, at least when not previously calibrated by suitable tests. Moreover, if an estimate needs previous experimental calibration, it cannot even be called a prediction, much less be safely used for such purposes under untested general load conditions. Structural engineers circumvent this issue using very generous safety factors in their designs (a factor of 10 or even 20 in desired fatigue lives is not uncommon), but this practice is at least uneconomical. Besides, it cannot be used in structural integrity evaluations, where actual safety factors must be calculated, not assumed. If PICC may not be the dominant FCG mechanism, this doubt alone certainly justifies the careful experimental verification of the actual relevance of ΔK_{eff} in relatively simple and easily reproducible unambiguous FCG tests, like those presented in the following.

EXPERIMENTAL SETUP

The objective of this work is to use simple and easily reproducible fatigue tests to identify if ΔK_{eff} really is its FCG driving force. Needless to say, to measure ΔK_{eff} properly, reliably, and accurately is a necessary condition to do so. This is the reason for choosing to propagate fatigue cracks in standard DC(T) and C(T) specimens [14] under fixed $\{\Delta K, K_{max}\}$ conditions, continuously measuring FCG rates da/dN and opening SIFs K_{op} along the entire crack path. To calculate ΔK and K_{max} , the crack length is measured by the traditional compliance technique, using a strain gage bonded on the back face of the specimens and standard ASTM SIF equations. Moreover, crack length measurements are frequently verified by optical means as the cracks grow during the FCG tests. The loads are controlled by a closed loop system to maintain quasi-constant $\{\Delta K, K_{max}\}$ conditions (according to ASTM E647 procedures [15]). Finally, special care is taken to avoid any O.L.s during the entire FCG process in all tests. Hence, there is no mystery in such simple tests. They only need to use traditional laboratorial procedures with proper care. That is why it is claimed above that these tests are easily reproducible. Nevertheless, it is worth to mention some of the tricks used to improve the quality of the tests, as follows.

To verify whether ΔK_{eff} really controls FCG rates in any test, it is indispensable to measure directly the opening loads K_{op} , preferably using the very same compliance technique used by Elber to identify them (Fig. 2a). However, since there are controversies about where to measure K_{op} (some experts claim K_{op} should be measured by transducers located near the crack tip [16]), both near (to the crack tip) and far (from it) redundant strain measurements are used in this work. Traditional electrical resistance strain gages, the most reliable strain transducers, are used to measure K_{op} during the load cycle of the FCG specimens. The gage bonded to the back face of the specimen, used to measure crack length, is also used to measure the far-field compliance, and a strip with 10 parallel gages bonded along its residual ligament is used to measure the near-field strains (while the crack tip does not cut them).

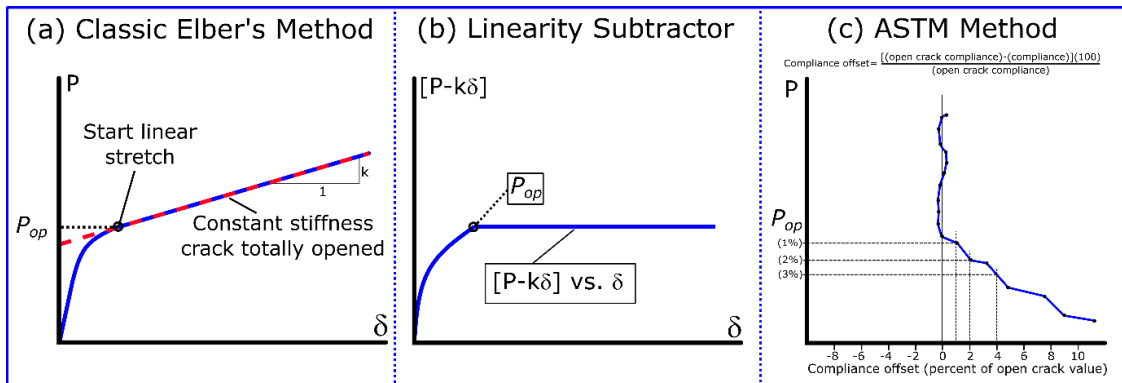


Figure 2: Methods used to measure the crack opening load P_{op} : (a) the classic Elber's method, (b) the linearity subtractor technique, and (c) the ASTM method.

To enhance the resolution of the opening loads and to improve the accuracy of such measurements, Paris and Hermann proposed to subtract the linear part of the compliance signal and then to amplify the resulting difference (Fig. 2b). Their idea was successfully used in the analog linearity subtractor described a long time ago, which could identify K_{op} within 1% of K_{max} [17]. The same idea is digitally adapted to identify K_{op} in the tests reported here. Additionally, an independent digital image correlation (DIC) system is used to obtain two other types of redundant K_{op} measurements (and to verify the crack length). This precaution may be over-conservative and even unnecessary, but it is used here because ΔK_{eff} issues are frequently treated in an emotional way in the literature, so it is better to be safe than sorry when dealing with them. Anyway, since the DIC system was already available and its operational cost involves only man-hours, these additional measurements certainly are at least an interesting way to verify the traditional compliance procedures.

Such redundant testing methodology was first used to verify if ΔK_{eff} controlled the FCG behavior of 1020 steel specimens, a body-centered cubic material, as reported in [9, 10]. The main conclusion of those tests was that FCG rates were not controlled by ΔK_{eff} , since the measured K_{op} significantly decreased (and thus the applied ΔK_{eff} increased) as the cracks grew longer, while the measured FCG rate (induced by fixed $\{\Delta K, K_{max}\}$ loading conditions) remained essentially constant, see Fig. 3. It is interesting to point out that these experimental results support the procedures recommended by the ASTM E647 standard test method for measurement of fatigue crack growth rates under a fixed R , which assumes they are caused by ΔK , not by ΔK_{eff} .

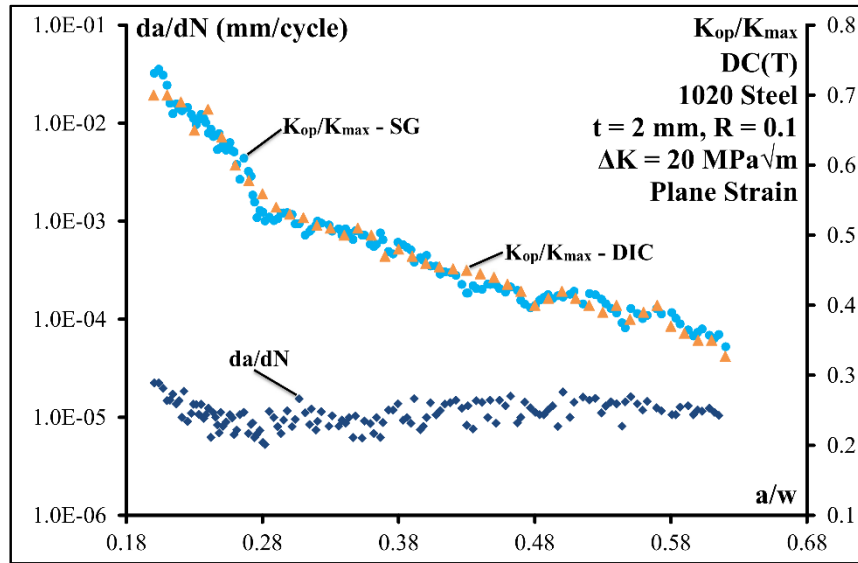


Figure 3: FCG rates da/dN and crack opening ratios K_{op}/K_{max} continuously measured under quasi-constant loading conditions (namely $\{\Delta K = 20\text{MPa}\sqrt{\text{m}}, R = 0.1\}$), by the four redundant techniques (near and far-field strain gages and DIC-based COD and strain fields) along the crack path in the thin DC(T) specimen ($t = 2\text{mm}$) of 1020 steel, supposedly under plane stress conditions [10].

Moreover, it is important to point out that such results are also very reassuring for structural engineers who must estimate residual FCG lives in practical applications. It is common practice to integrate FCG curves based on $\{\Delta K, K_{max}\}$ driving forces to calculate such lives [18], a technique that would be inappropriate if ΔK_{eff} was the actual cause for FCG. In fact, as discussed in [10], the main issue with the ΔK_{eff} concept is how to use it in practice. Whereas SIFs and thus SIF ranges ΔK can be calculated by standard stress analysis techniques, there is no foolproof universal method yet to reliably calculate K_{op} and consequently ΔK_{eff} in the complex structural components engineers must deal with. Indeed, while there are many catalogues of K -solutions, see e.g. [19], ΔK_{eff} cannot be listed because they are not unique for a given cracked body geometry. Since only simplified models are available to estimate K_{op} values based on an idealized behavior of very simple geometries, this is indeed a major problem for ΔK_{eff} -based FCG predictions.

The purpose of this work is to verify whether the same “ da/dN is not controlled by ΔK_{eff} ” conclusion observed in 1020 steel specimens holds for a face-centered cubic material as well. To do so, FCG tests are made on 6351-T6 Al specimens of two different geometries: disk-shaped compact tension DC(T) and compact tension C(T) specimens with two different thicknesses, 2 and 30mm, to simulated plane stress and plane strain conditions, respectively. All specimens were cut from the same 76mm-diameter bar with yield and ultimate strengths $S_Y = 170$ and $S_U = 290\text{MPa}$. The dimensions of these specimens are shown in Fig. 4, which lists as well the chemical composition of the Al 6351-T6 tested in this work.

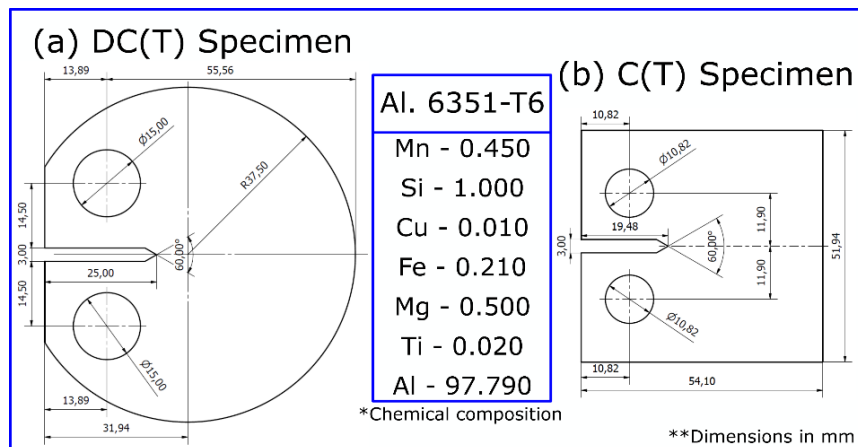


Figure 4: Dimensions of the (a) DC(T) and (b) C(T) specimens and the chemical composition of the tested 6351-T6 Al alloy.

Since all specimens are loaded under quasi-constant $\Delta K = 15\text{MPa}\sqrt{\text{m}}$ and $R = 0.1$ conditions, their thicknesses t are chosen to have nominally plane stress conditions in the thin $t = 2\text{mm}$ specimens (making the plastic zone that always

follows the fatigue crack tips $p_z > t$) and plane strain conditions in the thicker $t = 30\text{mm}$ ones. This choice assumes the classic ASTM E399 plane strain requirements can be used in FCG as well if $t > 2.5 \cdot (K_{max}/S_Y)^2$ [14]. Indeed, using Irwin's estimate for the p_z ahead of the crack tip, assuming this traditional 2D view is appropriate to define a plane stress state in FCG too, then if $t = 2\text{ mm}$, $p_{z_{max}} = (1/\pi) \cdot (K_{max}/S_Y)^2 = (1/\pi) \cdot [15/(0.9 \cdot 170)]^2 = 3.05\text{mm} > t$. On the other hand, specimens with $t = 30\text{mm}$ have $t > 2.5 \cdot (K_{max}/S_Y)^2 = 2.5 \cdot [15/(0.9 \cdot 170)]^2 = 24\text{mm}$, so they should grow their fatigue cracks under nominally plane strain conditions. This detail is important because if ΔK_{eff} is the FCG driving force then one could expect lower K_{op} and thus higher da/dN FCG rates under plane strain conditions. If, on the other hand, $\{\Delta K, K_{max}\}$ are the FCG driving forces, then no such difference is expected, since they are thickness-independent.

A custom-made closed loop control system is used to maintain the quasi-constant $\{\Delta K = 15\text{MPa}\sqrt{\text{m}}, R = 0.1\}$ loading conditions in all tests (according to ASTM E647 procedures). As mentioned above, this system uses the compliance technique to measure crack sizes from the signal of a strain-gage bonded on the back face of the specimens. This gage is continuously monitored through a Labview program [20] especially developed to control the P_{max} and $P_{min} = 0.1 \cdot P_{max}$ loadings applied to the specimen. In addition, this program also generates the FCG rate charts in real time. The crack opening SIF K_{op} is redundantly measured using the strain gage bonded on the back face of the specimen, a strip with a series of 10 strain gages bonded along the crack growth path, and an independent commercial DIC system from Correlated Solutions. This system measures displacement/strain fields on the specimen surface, see Fig. 5. The stereoscopic system consisted of two 5-MP Point Grey GRAS-50S5M CCD cameras with high magnification lenses (Tamron SPAF180mm F/3.5), an adjustable double fiber-optic light source, calibration grids, a suitable data acquisition system, and the software VIC-3D [21-22]. The DIC analysis used a subset size of 31×31 pixels, a grid step of 7 pixels and a strain window of 15×15 displacement points. The pixel size was approximately $9.3\ \mu\text{m}$. To avoid any doubts, the crack opening load is obtained from the DIC data by two independent methods. First, from the strain values measured at a point located 1mm in front of the crack tip. Second, from the crack opening displacements (COD) measured above and below the crack faces at points located 2mm behind the crack tip, see Fig. 5. Moreover, the experimental data from the strain gages and from the DIC analyses are used to locate the crack opening load P_{op} by three methods: the classic Elber's method [1], the linearity subtractor technique [17], and the ASTM method [15], see Fig. 2. Finally, the experimental setup is shown in Fig. 6.

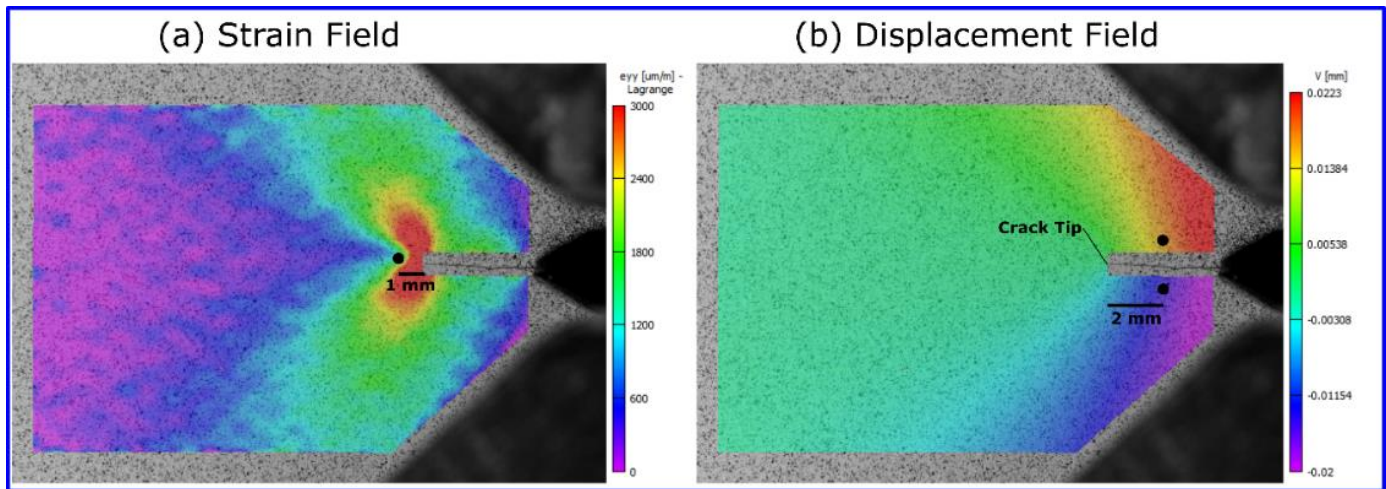


Figure 5: (a) Vertical displacement and (b) strain fields, obtained from the VIC 3-D DIC analysis.

EXPERIMENTAL RESULTS AND DISCUSSION

Figure 7 shows data obtained from two thin $t = 2\text{mm}$ DC(I) 6351-T6 Al specimens (Sp-1 and Sp-2), tested under nominally plane stress FCG conditions. It plots FCG rates da/dN and crack opening ratios K_{op}/K_{max} measured along the crack path under quasi-constant $\{\Delta K = 15\text{MPa}\sqrt{\text{m}}, R = 0.1\}$ loading conditions by four redundant techniques, near and far-field strain gages (SG), and DIC-based COD and strain fields. Figure 8 is similar, but it presents data from two thick specimens ($t = 30\text{mm}$) tested under nominally plane-strain FCG conditions.

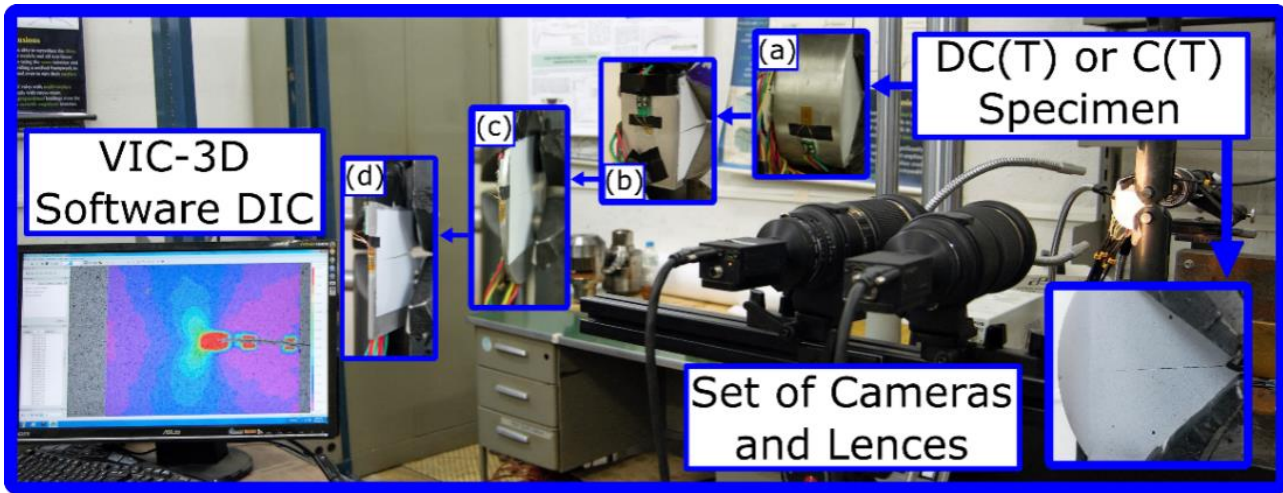


Figure 6: Experimental setup used to measure displacement fields on the specimen surface with the DIC system, with a strain field resulting from it in the lower left figure. Four types of specimens are used in this work: (a) plane strain DC(T), (b) plane strain C(T), (c) plane stress DC(T), and (d) plane stress C(T). Notice the back face strain gages bonded on them.

Figures 7 and 8 depict the evolution of the FCG rates and of the crack opening ratios K_{op}/K_{max} measured along the crack growth process. Notice that the K_{op} results obtained from the strain gage readings and from DIC analyses have the same trend along the entire crack path. These experimental results clearly show that the crack opening ratio K_{op}/K_{max} , like in the previous 1020 steel tests [9,10], significantly decreases as the crack length increases while the FCG rate remains practically constant during the entire tests. Thus, these data clearly contradict as well Elber's hypothesis that the effective stress intensity factor ΔK_{eff} would be the actual fatigue crack driving force. Moreover, these data suggest that this fact is material-independent, a strong evidence the widespread belief in the ΔK_{eff} hypothesis should be re-evaluated.

To avoid any doubts about the property of testing non-standard FCG DC(T) specimens (such specimens are accepted by the ASTM E399 but not by the E647 standard), the same tests were also carried out in standard C(T) specimens under the same constant $\{\Delta K = 15 \text{MPa}\sqrt{\text{m}}, R = 0.1\}$ loading conditions, see Figures 9 and 10.

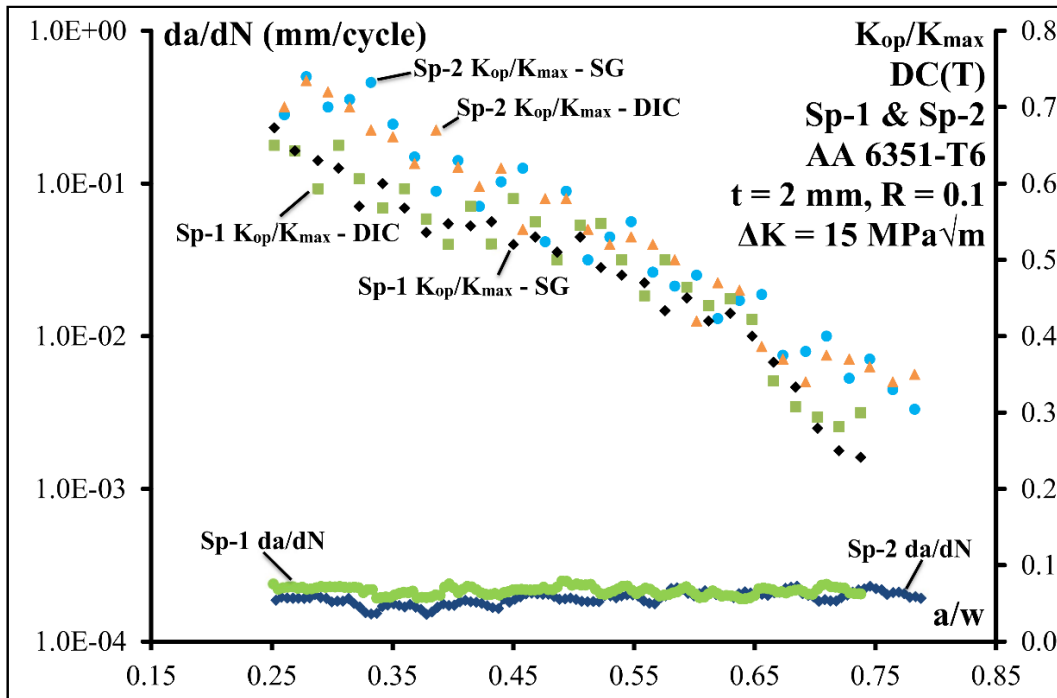


Figure 7: FCG rates da/dN and crack opening ratios K_{op}/K_{max} measured under $\{\Delta K = 15 \text{MPa}\sqrt{\text{m}}, R = 0.1\}$ quasi-constant loading conditions (according to ASTM E647 procedures) in two thin $t = 2 \text{mm}$ Al 6351-T6 DC(T) specimens (Sp-1 and Sp-2), tested under nominally plane-stress FGC conditions.

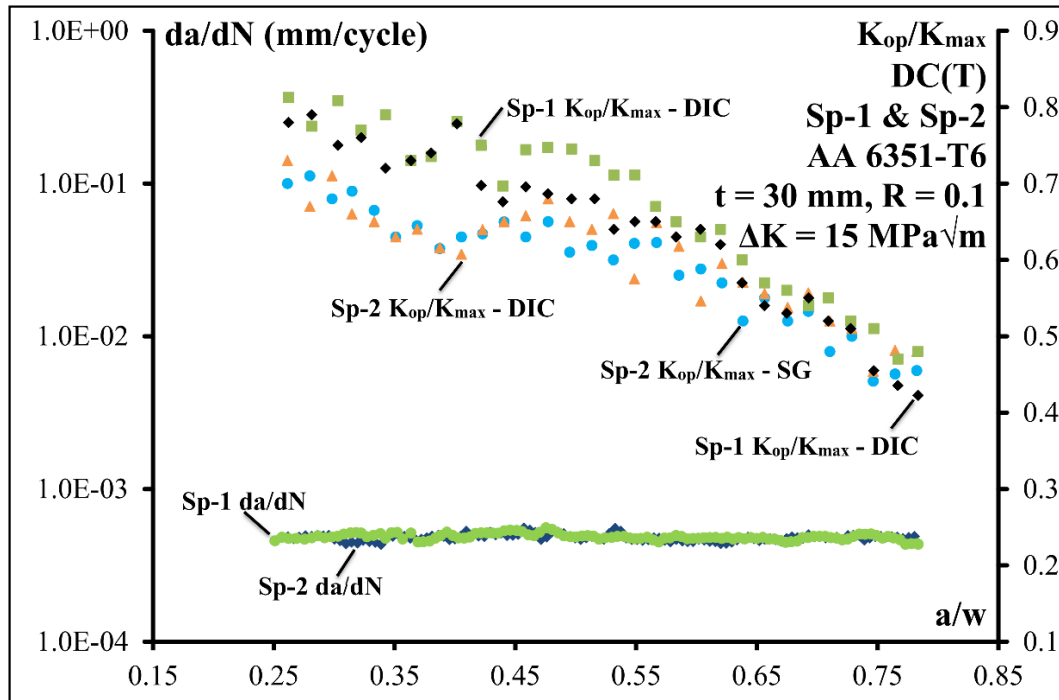


Figure 8: FCG rates da/dN and crack opening ratios K_{op}/K_{max} measured under $\{\Delta K = 15\text{MPa}\sqrt{\text{m}}, R = 0.1\}$ quasi-constant loading conditions (according to ASTM E647 procedures) in two thick $t = 30\text{mm}$ Al 6351-T6 DC(T) specimens (Sp-1 and Sp-2), tested under nominally plane-strain FGC conditions.

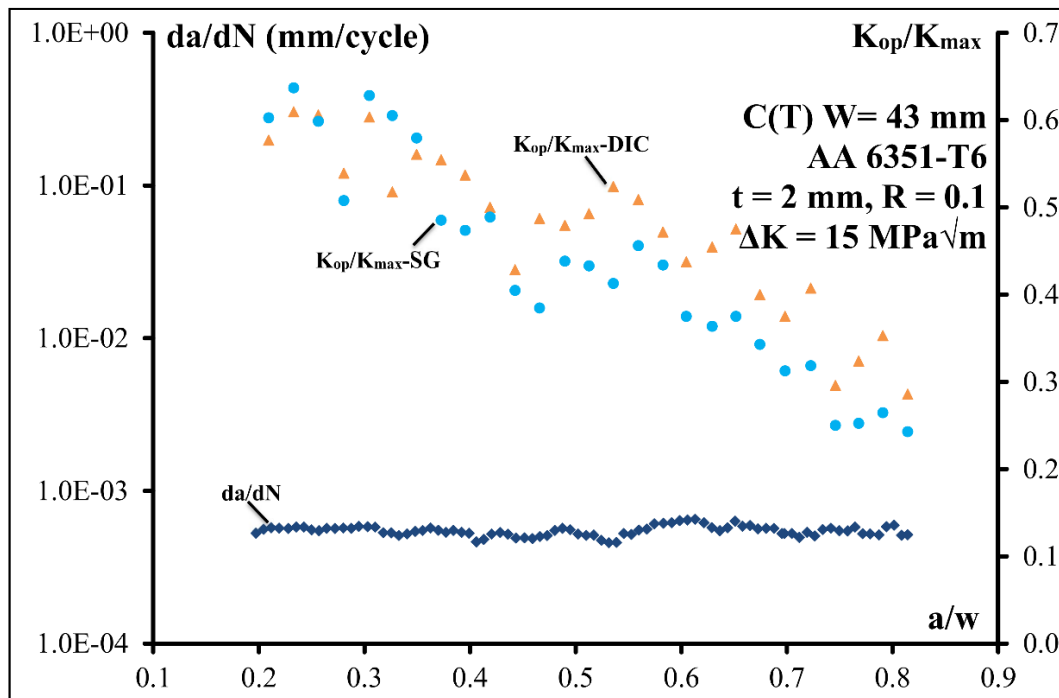


Figure 9: Results obtained by testing one $t = 2\text{mm}$ Al 6351-T6 C(T) specimen under nominally plane-stress conditions. FCG rates da/dN and crack opening ratios K_{op}/K_{max} measured under quasi-constant $\{\Delta K = 15\text{MPa}\sqrt{\text{m}}, R = 0.1\}$ loads.

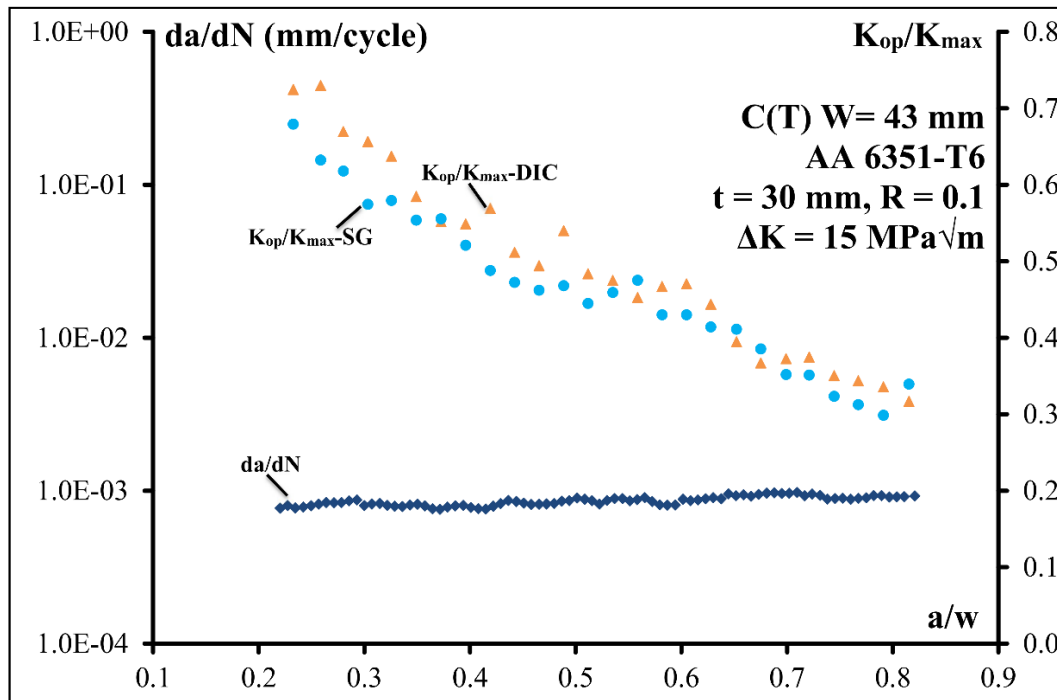


Figure 10: Results obtained by testing one $t = 30\text{mm}$ Al 6351-T6 C(T) specimen under nominally plane-strain conditions. FCG rates da/dN and crack opening ratios K_{op}/K_{max} measured under quasi-constant $\{\Delta K = 15\text{MPa}\sqrt{\text{m}}, R = 0.1\}$ loads.

The difference in the specimen type should not be an issue, because in principle FCG rates could be measured in any type of specimen whose SIF is known, since they are intended to be used in any structural component. Anyway, the data obtained from the C(T) specimens show once again the very same behavior of the crack opening ratio K_{op}/K_{max} . Indeed, it significantly decreases as the crack length increases, while the FCG rate remains practically constant during the entire tests, both in plane stress and in plane strain. Needless to say, these data once again clearly contradict Elber's hypothesis that the effective stress intensity factor ΔK_{eff} would be the actual fatigue crack driving force. Moreover, these results suggest that this conclusion is geometry-independent as well.

It must be pointed out that the data presented in this and in the previous works [9-10] show that the measured K_{op} behavior is not identical in all tested specimens. This indicates that K_{op} is not a property of the geometry/load pair. Instead, it can vary in nominally identical specimens submitted to equal loading conditions not only with the relative crack size a/w , but it can also depend on local details along the crack path, probably because it is affected by non-plasticity induced closure mechanisms. This K_{op} variation is still another reason to question the blind use of FCG models that assume ΔK_{eff} is the driving force in all fatigue problems.

Finally, it is worth to mention that there is a small difference between the FCG rates obtained in DC(T) and C(T) specimens. There is also an even smaller difference between the FCG rates measured in thin and thick specimens. A similar behavior was reported by Forth et al. in FCG tests performed under constant load conditions, when they tested C(T), M(T), and ESE(T) specimens, using the same material as well as specimen width (w) and thickness (t) [23, 24]. They concluded that the differences observed in FCG rates were probably caused by environmental effects and roughness of the crack faces, which could explain the variation reported in these results. However, such hypotheses are beyond the scope of this paper, thus they are not checked in this work.

CONCLUSIONS

After reviewing the basic arguments that either support or question Elber's classic hypothesis that FCG is driven by ΔK_{eff} , fatigue tests were performed to experimentally check it, in an attempt to verify whether ΔK_{eff} can indeed be assumed as the driving force for FCG in all situations. To do so, FCG rates da/dN and crack opening loads K_{op} were redundantly measured on FCG tests under quasi-constant ΔK and R conditions, enforced by an especially designed closed loop control system, in thin and thick DC(T) and C(T) AA 6351-T6 specimens to simulate nominally plane-stress and plane-strain FCG conditions. The opening loads were measured by Elber's compliance techniques, using as well the Paris and

Hermann linearity subtractor technique to enhance the K_{op} identification, and by the ASTM method. A series of strain gages bonded along the crack growth path, one strain gage bonded on the back face of the specimen, and COD and strain-based DIC techniques were all used to identify K_{op} by far and by near field measurements. The decreasing behavior of the crack opening ratio K_{op}/K_{max} obtained by these 4 redundant methods showed no discrepancy in the testing results, confirming the reliability and repeatability of the data obtained in previous works. Since the ΔK_{eff} measured along those tests augmented significantly with the crack size, whereas the measured FCG rates da/dN remained practically constant, it can be concluded that Elber's effective stress intensity factor range is not the actual FCG driving force for the analyzed tests.

ACKNOWLEDGEMENTS

Julián Andrés Ortiz González would like to gratefully acknowledge the support received from PUC-Rio.

REFERENCES

- [1] Elber, W. (1971). The significance of fatigue crack closure. ASTM STP 486, pp. 230-242. DOI: 10.1520/STP26680S.
- [2] Elber, W. (1970). Fatigue crack closure under cyclic tension. *Engineering Fracture Mechanics*, 2(1), pp. 37-45. DOI: 10.1016/0013-7944(70)90028-7
- [3] Ferreira, SE; Castro, JTP; Meggiolaro, MA. (2018). Fatigue crack growth predictions based on damage accumulation ahead of the crack tip calculated by strip-yield procedures. *International Journal of Fatigue*, 115, p.p. 89-106. DOI: 10.1016/j.ijfatigue.2018.03.001.
- [4] Ferreira, SE; Castro, JTP; Meggiolaro, MA; Miranda, ACO. Crack closure effects on fatigue damage ahead of crack tips. *International Journal of Fatigue*, under review.
- [5] Kemp, PMJ. (1990). Fatigue crack closure – a review. TR90046, Royal Aerospace Establish.
- [6] Skorupa, M. (1999). Load interaction effects during fatigue crack growth under variable amplitude loading - a literature review part II: qualitative interpretation. *Fatigue & Fracture of Engineering Materials & Structures*, 22(10) pp. 905 – 926. DOI: 10.1046/j.1460-2695.1999.00158.x.
- [7] Williams, JJ; Yazzie, KE; Padilla, E; Chawla, N; Xiao, X; de Carlo, F. (2013). Understanding fatigue crack growth in aluminum alloys by in situ X-ray synchrotron tomography. *International Journal of Fatigue*, 57, pp. 79-85. DOI: 10.1016/j.ijfatigue.2012.06.009.
- [8] Castro, JTP; Meggiolaro, MA; Miranda, ACO. (2005). Singular and non-singular approaches for predicting fatigue crack growth behavior. *International Journal of Fatigue*, 27 (10-12), pp. 1366-1388. DOI: 10.1016/j.ijfatigue.2005.07.018.
- [9] Castro, JTP; Meggiolaro, MA; González, JAO. (2015). Can ΔK_{eff} be assumed as the driving force for fatigue crack growth? *Frattura ed Integrità Strutturale*, 33, pp. 97-104. DOI: 10.3221/IGF-ESIS.33.13.
- [10] González, JAO; Castro, JTP; Gonzales, GLG; Meggiolaro, MA; Freire, JLF. (2017). On DIC measurements of ΔK_{eff} to verify if it is the FCG driving force. *Frattura ed Integrità Strutturale*, 41, pp. 227-235. DOI: 10.3221/IGF-ESIS.41.31.
- [11] Chen, DL; Weiss, B; Stickler, R. (1994). The effective fatigue threshold: significance of the loading cycle below the crack opening load. *International Journal of Fatigue*, 16(7), pp. 485-491. DOI: 10.1016/0142-1123(94)90199-6.
- [12] Vasudevan, AK; Sadananda, K; Holtz, RL. (2005). Analysis of vacuum fatigue crack growth results and its implications. *International Journal of Fatigue*, 27(10-12), pp.1519-1529. DOI: 10.1016/j.ijfatigue.2005.07.026.
- [13] Vasudevan, AK; Sadananda, K; Louat, NA. (1994). Review of crack closure, fatigue crack threshold and related phenomena. *Materials Science and Engineering*, 188(1-2), pp. 1–22. DOI: 10.1016/0921-5093(94)90351-4.
- [14] ASTM E399. (2013). Standard test method for linear-elastic plane-strain fracture toughness K_{Ic} of metallic materials. ASTM Standards 03.01.
- [15] ASTM E647. (2013). Standard test method for measurement of fatigue crack growth rates. ASTM Standards 03.01.
- [16] Yamada, Y; Newman Jr., JC. (2009). Crack closure under high load-ratio conditions for Inconel-718 near threshold behavior. *Engineering Fracture Mechanics*, 76 (2), pp. 209-220. DOI: 10.1016/j.engfracmech.2008.09.009.
- [17] Castro, JTP. (1993). A circuit to measure crack closure. *Experimental Techniques*, 17(2), pp. 23-25. DOI: 10.1111/j.1747-1567.1993.tb00720.
- [18] Castro, JTP and Meggiolaro, MA. (2016). *Fatigue Design Techniques*, vol. 3: Crack Propagation, Temperature and Statistical Effects. USA: CreateSpace, 110-110.



- [19] Tada, H; Paris, PC; Irwin, GR. (2000). The Stress Analysis of Cracks Handbook. London: ASME Press, pp. 10-50. DOI: 10.1115/1.801535.
- [20] National Instruments, Labview. Available at: <http://www.ni.com/en-us/shop/labview.html> [access Feb 10, 2019].
- [21] Correlated Solutions, VIC-3D. Available at: <https://www.correlatedsolutions.com/vic-3d> [access Feb 10, 2019].
- [22] Sutton, MA; Orteu, JJ; Schreier, H. (2009). Image Correlation for Shape, Motion and Deformation Measurements. Springer, pp. 20-50.
- [23] Forth SC; Johnston WM; Seshadri BR. (2006). The Effect of the Laboratory Specimen on Fatigue Crack Growth Rate. Fracture of Nano and Engineering Materials and Structures, Springer, pp. 457-458. DOI: 10.1007/1-4020-4972-2_226.
- [24] Forth, SC; Newman, JC; Forman, RG. (2007). Anomalous Fatigue Crack Growth Data Generated Using the ASTM Standards. Fatigue and Fracture Mechanics, ASTM, 35, pp. 244-255. DOI:10.1520/STP45540S.